

Relativistic BCS-BEC crossover in a boson-fermion model

Jian Deng^{1,*} Andreas Schmitt^{2,†} and Qun Wang^{1,‡}

¹*Department of Modern Physics, University of Science and Technology of China, Anhui 230026, People's Republic of China*

²*Department of Physics, Washington University St Louis, MO 63130, USA*

(Dated: November 28, 2006)

We investigate the crossover from Bardeen-Cooper-Schrieffer (BCS) pairing to a Bose-Einstein condensate (BEC) in a relativistic superfluid within a boson-fermion model. The model includes, besides the fermions, separate bosonic degrees of freedom, accounting for the bosonic nature of the Cooper pairs. The crossover is realized by tuning the difference between the boson mass and boson chemical potential as a free parameter. The model yields populations of condensed and uncondensed bosons as well as gapped and ungapped fermions throughout the crossover region for arbitrary temperatures. Moreover, we observe the appearance of antiparticles for sufficiently large values of the crossover parameter. The model can potentially be applied to color superconductivity in dense quark matter at strong couplings.

PACS numbers: 12.38.Mh,11.10.Wx,03.75.Nt

I. INTRODUCTION

An arbitrarily weak attractive interaction between fermions in a many-fermion system leads to the formation of Cooper pairs. This phenomenon is well described within Bardeen-Cooper-Schrieffer (BCS) theory [1]. In this situation, Cooper pairs are typically of a size much larger than the mean interparticle distance. The picture changes for sufficiently large interaction strengths. In this case, Cooper pairs become bound states, and superfluidity is realized by a Bose-Einstein condensation (BEC) of molecular bosons composed of two fermions. A crossover between the weak-coupling BCS regime and the strong-coupling BEC regime is expected [2].

Experimentally, this crossover has been studied in systems of cold fermionic atoms in a magnetic trap, where the coupling strength can be tuned around a Feshbach resonance with the help of an external magnetic field [3]. Recently, these studies have been extended to the case two fermion species with imbalanced populations [4]. In this case, the crossover is most likely replaced by one or more phase transitions, and the appearance of exotic superfluids seems to be a very interesting possibility [5].

Besides the nonrelativistic atomic systems, there is also a strong motivation to study the relativistic BCS-BEC crossover. One possible realization is pion condensation, which, for large isospin densities, crosses over into Cooper pairing of quarks and antiquarks [6]. Another possibility is dense quark matter which may be present in compact stars [7]. Under astrophysical conditions of densities of a few times the nuclear ground state density and comparably small temperatures of 1 MeV and lower, quark matter is a color superconductor [8, 9]. Analogous to electrons in a metal or alloy or fermionic atoms in a magnetic trap, quarks form Cooper pairs due to an attractive interaction, here mediated by gluon exchange. Because of asymptotic freedom, color superconductivity at asymptotically large densities can be studied in a weak-coupling approach using perturbative methods within QCD [10, 11]. However, for moderate densities as present in compact stars, the validity of these results is questionable. More phenomenological models such as the Nambu-Jona-Lasinio (NJL) model, have therefore been employed, mimicking the gluon exchange by a pointlike interaction between the quarks (see Ref. [12] and references therein). Both QCD and NJL approaches usually are applied within a BCS-like picture. However, quark matter in compact stars may well be in a strong-coupling regime where a BEC-like picture is more appropriate [13, 14, 15, 16].

The model employed in this paper is too simple to describe a realistic scenario of color-superconducting quark matter since it contains only a single fermion species and therefore is unable to account for different pairing patterns of quarks. Therefore, it also cannot account for a possible mismatch in Fermi momenta of the constituents of a Cooper pair. This is an unavoidable complication in realistic color and electrically neutral color superconductors [17]. However, our model can certainly be extended to include these effects.

*Electronic address: djdddd@mail.ustc.edu.cn

†Electronic address: aschmitt@wuphys.wustl.edu

‡Electronic address: qunwang@ustc.edu.cn

In order to describe the crossover from BCS to BEC we shall not consider a purely fermionic model which may describe this crossover as a function of the fermionic coupling strength. We rather set up a theory with bosonic and fermionic degrees of freedom. Here, fermions and bosons are coupled through a Yukawa interaction and required to be in chemical equilibrium, $2\mu = \mu_b$, where μ and μ_b are the fermion and boson chemical potentials, respectively. We treat the (renormalized) boson mass $m_{b,r}$ and the boson-fermion coupling g as free parameters. Then, tuning the parameter $x = -(m_{b,r}^2 - \mu_b^2)/(4g^2)$ drives the system from the BCS to the BEC regime. The fermionic chemical potential shall be self-consistently determined from the gap equation and charge conservation. This picture is inspired by the boson-fermion model of superconductivity considered in Ref. [18], which has been used in the context of cold fermionic atoms [19]. It also has possible applications for high-temperature superconductivity [20]. For simplicity, we shall restrict ourselves to the evaluation of the model in a mean-field approximation.

Our convention for the metric tensor is $g^{\mu\nu} = \text{diag}(1, -1, -1, -1)$. Our units are $\hbar = c = k_B = 1$. Four-vectors are denoted by capital letters, $K \equiv K^\mu = (k_0, \mathbf{k})$ with $k = |\mathbf{k}|$. Fermionic Matsubara frequencies are $\omega_n = ik_0 = (2n + 1)\pi T$, while bosonic ones are $\omega_n = ik_0 = 2n\pi T$ with the temperature T and n an integer.

II. THE BOSON-FERMION MODEL FOR A RELATIVISTIC SUPERFLUID

A. Setting up the model

We use a model of fermions and composite bosons coupled to each other by a Yukawa interaction. The Lagrangian is given by a free fermion part \mathcal{L}_f , a free boson part \mathcal{L}_b and an interaction part \mathcal{L}_I ,

$$\mathcal{L} = \mathcal{L}_f + \mathcal{L}_b + \mathcal{L}_I, \quad (1)$$

with

$$\mathcal{L}_f = \bar{\psi}(i\gamma^\mu \partial_\mu + \gamma_0 \mu - m)\psi, \quad (2a)$$

$$\mathcal{L}_b = |(\partial_t - i\mu_b)\varphi|^2 - |\nabla\varphi|^2 - m_b|\varphi|^2, \quad (2b)$$

$$\mathcal{L}_I = g(\varphi\bar{\psi}_C i\gamma_5 \psi + \varphi^* \bar{\psi} i\gamma_5 \psi_C). \quad (2c)$$

The fermions are described by the spinor ψ , while the bosons are given by the complex scalar field φ . The charge conjugate spinors are defined by $\psi_C = C\bar{\psi}^T$ and $\bar{\psi}_C = \psi^T C$ with $C = i\gamma^2\gamma^0$. The fermion (boson) mass is denoted by m (m_b). We choose the boson chemical potential to be twice the fermion chemical potential,

$$\mu_b = 2\mu. \quad (3)$$

Therefore, the system is in chemical equilibrium with respect to the conversion of two fermions into one boson and vice versa. This allows us to model the transition from weakly-coupled Cooper pairs made of two fermions into a molecular dfermionic bound state, described as a boson. The interaction term accounts for a local interaction between fermions and bosons with coupling constant g . In order to describe BEC of the bosons, we have to separate the zero mode of the field φ [21]. Moreover, we shall replace this zero-mode by its expectation value

$$\phi \equiv \langle \varphi_0 \rangle \quad (4)$$

and neglect the interaction between the fermions and the *non-zero* boson modes. This corresponds to the mean-field approximation. Then, with the Nambu-Gorkov spinors

$$\Psi = \begin{pmatrix} \psi \\ \psi_C \end{pmatrix}, \quad \bar{\Psi} = (\bar{\psi}, \bar{\psi}_C), \quad (5)$$

the Lagrangian can be written as

$$\mathcal{L} = \frac{1}{2}\bar{\Psi}\mathcal{S}^{-1}\Psi + [(2\mu)^2 - m_b^2]|\phi|^2 + |(\partial_t - 2i\mu)\varphi|^2 - |\nabla\varphi|^2 - m_b^2|\varphi|^2. \quad (6)$$

Note that we have dropped the mixing terms of zero and non-zero boson modes since they vanish when carrying out the path integral. Here \mathcal{S}^{-1} is the inverse fermion propagator which reads in momentum space

$$\mathcal{S}^{-1}(P) = \begin{pmatrix} P_\mu \gamma^\mu + \mu \gamma_0 - m & 2ig\gamma_5 \phi^* \\ 2ig\gamma_5 \phi & P_\mu \gamma^\mu - \mu \gamma_0 - m \end{pmatrix}. \quad (7)$$

It is instructive to compare this form of the propagator to the corresponding one in a purely fermionic model, see for instance Ref. [14]. As expected, the Bose condensate is related to the diquark condensate Δ ,

$$\Delta = 2g\phi. \quad (8)$$

As we shall see below, cf. Eq. (11), Δ is the energy gap in the quasi-fermion excitation spectrum. In a purely fermionic model, $\Delta = 2G\langle\bar{\psi}_C i\gamma_5 \psi\rangle$, where G is the coupling constant related to the interaction between the fermions. Note that G has mass dimension -2 , while our boson-fermion coupling g is dimensionless. Therefore, g does not play the role of the crossover parameter, as G does in the fermionic model. We shall explain this in more detail in Sec. II C.

B. Thermodynamic potential

In order to obtain the thermodynamical potential density Ω , we compute the partition function

$$\mathcal{Z} = \int [d\Psi][d\bar{\Psi}][d\varphi][d\varphi^*] \exp \left[\int_0^{1/T} d\tau d^3x \mathcal{L} \right], \quad (9)$$

where T is the temperature, and \mathcal{L} is the Lagrangian in the mean field approximation given in Eq. (6). The thermodynamic potential density is then obtained from $\Omega = -T/V \ln \mathcal{Z}$, where V is the volume of the system. One obtains after performing the path integral and the sum over Matsubara frequencies,

$$\begin{aligned} \Omega = & - \sum_{e=\pm} \int \frac{d^3k}{(2\pi)^3} \left\{ \epsilon_k^e + 2T \ln \left[1 + \exp \left(-\frac{\epsilon_k^e}{T} \right) \right] \right\} \\ & + \frac{[m_b^2 - (2\mu)^2]\Delta^2}{4g^2} + \frac{1}{2} \sum_{e=\pm} \int \frac{d^3k}{(2\pi)^3} \left\{ \omega_k^e + 2T \ln \left[1 - \exp \left(-\frac{\omega_k^e}{T} \right) \right] \right\}. \end{aligned} \quad (10)$$

We have used Eq. (8) and denoted the quasi-particle energy for fermions ($e = +1$) and antifermions ($e = -1$) by

$$\epsilon_k^e = \sqrt{(\epsilon_{k0} - e\mu)^2 + \Delta^2}, \quad \epsilon_{k0} = \sqrt{k^2 + m^2}, \quad (11)$$

and the (anti)boson energy by

$$\omega_k^e = \sqrt{k^2 + m_b^2} - e\mu_b. \quad (12)$$

Furthermore, we have assumed Δ (and thus ϕ) to be real.

C. Crossover parameter

We shall now define the crossover parameter whose variation carries the system from the BCS to the BEC regime. Let us first recall the corresponding crossover parameter in a purely fermionic model. In this case, the fermionic coupling G has to be renormalized. This is in contrast to the weak-coupling regime where the gap equation is well-defined with the bare coupling G (a natural cutoff is provided by the Debye frequency in the non-relativistic case; in QCD, the gap is a function of momentum and peaks around the Fermi surface, providing a regular behavior of the gap equation). The renormalized coupling is proportional to the scattering length. In the context of cold fermionic atoms, the scattering length is the physical quantity which can be controlled upon tuning the external magnetic field. For the relativistic case, see Ref. [16] for the relation between the renormalized coupling and the scattering length. The definition of the crossover parameter in the present model goes along the same lines. Instead of a renormalized coupling we introduce the renormalized boson mass

$$m_{b,r}^2 = 4g^2 \frac{\partial \Omega}{\partial \Delta^2} \Big|_{\Delta=\mu=T=0} = m_b^2 - 4g^2 \int \frac{d^3k}{(2\pi)^3} \frac{1}{\epsilon_{k0}}. \quad (13)$$

This allows us to define the (renormalized) crossover parameter

$$x \equiv -\frac{m_{b,r}^2 - (2\mu)^2}{4g^2}. \quad (14)$$

The parameter x can be varied from negative values with large modulus (BCS) to large positive values (BEC). In between, $x = 0$ is the unitary limit [22, 23, 24]. Therefore, $1/x$ behaves similar to the scattering length: the BCS (BEC) limit is approached via $1/x \uparrow 0$ ($1/x \downarrow 0$) while the unitary regime corresponds to $1/x = \pm\infty$.

We may thus write the thermodynamical potential in terms of the parameters (x, g) instead of the original pair (m_b, g) . To this end, we have to express the bare boson mass m_b in terms of x and g . With the help of Eqs. (13) and (14) we find

$$m_b^2 - (2\mu)^2 = 4g^2 \left(\int \frac{d^3 k}{(2\pi)^3} \frac{1}{\epsilon_{k0}} - x \right) \equiv 4g^2(x_0 - x). \quad (15)$$

For sufficiently small fermion masses, $m \ll \Lambda$, where Λ is the cutoff in the momentum integrals, we have

$$x_0 \simeq \frac{\Lambda^2}{4\pi^2}. \quad (16)$$

One sees from Eq. (15) that x_0 is an upper limit for x in order to ensure non-negative bosonic occupation numbers. Moreover, in the limit of large $x \rightarrow x_0$ the boson chemical potential approaches the (bare) boson mass, $\mu_b \rightarrow m_b$. The condition of Bose-Einstein condensation in a free bosonic system with fixed bosonic charge is $\mu_b = m_b$. In the present model, however, we shall observe a nonzero Bose condensate also for $\mu_b < m_b$, corresponding to $x < x_0$.

Having defined the crossover parameter x and its definition range $x \in [-\infty, x_0]$, we note that, within our simple model, we are left with the second free parameter g . We shall discuss below how the choice of g effects the behavior of the system in the BCS-BEC crossover. For most of our results we shall, however, use a single fixed value of g .

D. Densities and gap equation

Next, we derive the charge conservation equation and the gap equation which shall later be solved numerically. The total charge density

$$n = -\frac{\partial \Omega}{\partial \mu} \quad (17)$$

can, using Eq. (10), be written as

$$n = n_F + n_0 + n_B. \quad (18)$$

Here, the fermionic contribution is given by

$$n_F \equiv 2 \sum_{e=\pm} e \int \frac{d^3 k}{(2\pi)^3} \frac{\xi_k^e}{2\epsilon_k^e} [f_F(\epsilon_k^e) - f_F(-\epsilon_k^e)], \quad (19)$$

where we abbreviated

$$\xi_k^e \equiv \epsilon_{k0} - e\mu, \quad (20)$$

and f_F is the Fermi distribution function, $f_F(x) = 1/[\exp(x/T) + 1]$. The factor 2 in front of the sum in Eq. (19) originates from the two spin degrees of freedom. From Eq. (19) one recovers the limit case of a free Fermi gas at zero temperature,

$$n_F(\Delta = T = 0) = \frac{(\mu^2 - m^2)^{3/2}}{6\pi^2} [\Theta(\mu - m) - \Theta(-\mu - m)]. \quad (21)$$

The condensate density is

$$n_0 \equiv \frac{2\mu \Delta^2}{g^2}, \quad (22)$$

and the thermal boson contribution is

$$n_B \equiv 2 \sum_{e=\pm} e \int \frac{d^3 k}{(2\pi)^3} f_B(\omega_k^e), \quad (23)$$

where f_B is the Bose distribution function, $f_B(x) = 1/[\exp(x/T) - 1]$. The factor 2 in the boson densities originates from Eq. (3), i.e., from the fact that each boson is composed of two fermions. For the following, let us also define the charge fractions

$$\rho_{B/F} \equiv \frac{n_{B/F}}{n}, \quad \rho_0 \equiv \frac{n_0}{n}, \quad (24)$$

and an effective Fermi momentum p_F through

$$n = \frac{p_F^3}{3\pi^2}. \quad (25)$$

The effective Fermi energy is then given by $\epsilon_F \equiv \sqrt{p_F^2 + m^2}$. The various densities appearing on the right-hand side of Eq. (18) are interpreted as follows. The fermions that contribute to n_F are, for temperatures below the superfluid transition temperature, constituents of weakly coupled Cooper pairs. For temperatures larger than the transition temperature, n_F corresponds to free fermions. The bosons that contribute to the boson density n_B are, for all temperatures, *uncondensed* molecular bound states, composed of two fermions. Condensation of these pairs can only occur below the transition temperature and results in a nonzero condensate density n_0 .

In order to find the gap equation in the case of a fixed charge density, we have to minimize the free energy density

$$F = \Omega + \mu n. \quad (26)$$

Here, μ is an implicit function of n (and of the gap Δ) through Eq. (17). Minimization with respect to Δ yields

$$0 = \frac{dF}{d\Delta} = \frac{\partial\Omega}{\partial\Delta} + \frac{\partial\Omega}{\partial\mu} \frac{\partial\mu}{\partial\Delta} + n \frac{\partial\mu}{\partial\Delta} = \frac{\partial\Omega}{\partial\Delta}, \quad (27)$$

where Eq. (17) has been used. For $\Delta \neq 0$ Eq. (27) reads

$$-x = \sum_{e=\pm} \int \frac{d^3k}{(2\pi)^3} \left(\frac{1}{2\epsilon_k^e} \tanh \frac{\epsilon_k^e}{2T} - \frac{1}{2\epsilon_{k0}} \right). \quad (28)$$

III. RESULTS AND DISCUSSION

The two coupled equations (18) and (28) with the definitions (19), (22), and (23) shall be used in the following to determine the gap Δ , and the chemical potential μ as functions of the crossover parameter x , see Eq. (14), and the temperature T at fixed effective Fermi momentum p_F , fermion mass m , and boson-fermion coupling g . The solution $[\Delta(x, T), \mu(x, T)]$ can then, in turn, be used to compute the densities of fermions and bosons in the x - T plane. We shall present results for the zero-temperature case, Sec. III A, and at the critical temperature T_c , Sec. III B. Then, we show results for a fixed x and arbitrary temperature T , Sec. III C. Throughout these subsections, we shall fix

$$\frac{p_F}{\Lambda} = 0.3, \quad \frac{m}{\Lambda} = 0.2, \quad g = 4. \quad (29)$$

In Sec. III D we present the ratios Δ_0/μ_0 and T_c/Δ_0 for different values of m and g as a function of x . Here and in the following, we use the subscript 0 at Δ and μ to denote the zero-temperature value.

A. Zero temperature

For $T = 0$, there are no thermal bosons, $n_B = 0$, and Eqs. (18) and (28) become

$$n = n_F + n_0, \quad (30a)$$

$$-x = \sum_{e=\pm} \int \frac{d^3k}{(2\pi)^3} \left(\frac{1}{2\epsilon_k^e} - \frac{1}{2\epsilon_{k0}} \right), \quad (30b)$$

with the zero-temperature expressions for the fermion densities

$$n_F \equiv 2 \sum_{e=\pm} e \int \frac{d^3k}{(2\pi)^3} \frac{\xi_k^e}{2\epsilon_k^e}. \quad (31)$$

The numerical results for the solution of the coupled equations (30a) and (30b) are shown in Fig. 1. The left panel shows the fermion chemical potential μ_0 and the gap Δ_0 as functions of x . In the weak-coupling regime (small x) we see that the chemical potential is given by the Fermi energy, $\mu_0 = \epsilon_F$. For the given parameters, $\epsilon_F/\Lambda \simeq 0.36$. The chemical potential decreases with increasing x and approaches zero in the far BEC region. The gap is exponentially small in the weak-coupling region, as expected from BCS theory. It becomes of the order of the chemical potential around the unitary limit, $x = 0$, and further increases monotonically for positive x . In the unitary limit, we have $\mu/\epsilon_F \simeq 0.37$, while in nonrelativistic fermionic models $\mu/\epsilon_F \simeq 0.4 - 0.5$ was obtained [22, 23, 24].

The corresponding fermion and boson densities are shown in the right panel of Fig. 1. These two curves show the crossover: at small x all Cooper pairs are resonant states, which is characterized by a purely fermionic density, $n = n_F$; at large x , on the other hand, Cooper pairs are bound states and hence there are no fermions in the system. The charge density is rather dominated by a bosonic condensate, $n = n_0$. The crossover region is located around $x = 0$. We can characterize this region quantitatively as follows. We write the boson mass as $m_b = 2m - E_{\text{bind}}$. Then, a bound state appears for positive values of the binding energy E_{bind} , i.e., for $2m > m_b$. With Eq. (15) this inequality reads

$$\mu_0^2 < m^2 - g^2(x_0 - x). \quad (32)$$

Since μ_0 is a monotonically decreasing function of x , this relation suggests (note that $x_0 - x > 0$ by construction): (i) for sufficiently large $x < x_0$ bound states appear for any fixed g (ii) the larger g the “later” (= larger values of x) bosonic states appear. We have confirmed these two statements numerically by using different values of g . The value $g = 4$ is chosen such that there is an approximately balanced coexistence of fermions and bosons at $x = 0$, $n_F \simeq n_0$, as can be seen in the right panel of Fig. 1.

One may ask whether there is a contribution of antifermions to the total fermion charge. In the BCS regime there is a Fermi surface given by $\mu > 0$ and antifermion excitations are obviously suppressed. However, during the crossover, μ decreases and there might be the possibility of the appearance of antifermions. The contributions of fermions and antifermions to the total fermion charge seem to be given by the terms $e = +1$ and $e = -1$ in Eq. (31). A separate discussion of these terms is not straightforward because they contain divergent contributions which cancel in the sum but not in each term separately. Thus, a renormalization of both terms would be required. In the BCS regime, $x \rightarrow -\infty$, vacuum contributions $\propto \Lambda^3$ have to be subtracted. For nonzero values of the gap, however, more divergent terms appear, involving powers of both the cutoff and the gap. (Note that this problem is not unlike the one encountered in Ref. [25], where medium-dependent counter terms were introduced in the calculation of the Meissner mass. In fact, we shall choose a similar renormalization in the following calculation of the energy density.)

In any case, separate charges of fermions and antifermions are not measurable quantities since any potential experiment would solely measure the total charge. Therefore, we shall describe the onset of a nonzero antiparticle population in terms of the energy density. In this quantity, we expect the contributions from particles and antiparticles to add up, in contrast to the charge density where the contributions (partially) cancel each other.

Let us first discuss the quasi-fermion and quasi-antifermion excitation energies given by ϵ_k^+ and ϵ_k^- from Eq. (11). Inserting the numerical solutions for μ and Δ into these energies results in the curves shown in Fig. 2. These excitation energies show that, for large values of x , quasi-fermions and quasi-antifermions become degenerate due to the vanishingly small chemical potential. Because of the large energy gap, we expect neither quasi-fermions nor quasi-antifermions to be present in the system.

This statement can be made more precise and generalized to nonzero temperatures upon considering the energy density E . Using the thermodynamic potential density Ω from Eq. (10) and the entropy density $S = -\partial\Omega/(\partial T)$ we have $E = \Omega + \mu n + TS$. We obtain

$$E = E_F + E_B, \quad (33)$$

with the fermionic and bosonic contributions

$$E_F = - \sum_e \int \frac{d^3 k}{(2\pi)^3} \epsilon_k^e [1 - 2f_F(\epsilon_k^e)] + \mu n_F, \quad (34a)$$

$$E_B = \frac{1}{2} \sum_e \int \frac{d^3 k}{(2\pi)^3} \omega_k^e [1 + 2f_B(\omega_k^e)] + (x_0 - x)\Delta^2 + \mu(n_0 + n_B). \quad (34b)$$

The renormalization of the fermionic part can now be chosen such that there are no quasi-particles at $T = n_F = 0$, in accordance with the above argument. Hence we subtract the “vacuum contribution” $E_F(T = n_F = 0)$ to obtain the renormalized energy density

$$E_{F,r} = 2 \sum_e \int \frac{d^3 k}{(2\pi)^3} \epsilon_k^e f_F(\epsilon_k^e) + \mu n_F. \quad (35)$$

For $T = 0$, only the second term survives (remember that $\epsilon_k^e > 0$), and E_F behaves as shown in the left panel of Fig. 3. For nonzero temperatures, however, we see that there is a nonzero fermionic energy density even for $n_F = 0$. This is related to the excitation of quasi-antifermions, as we shall discuss in the next subsection.

For the bosonic energy density, we subtract the analogous vacuum part $E_B(T = n_0 + n_B = 0)$. Hence we obtain the renormalized energy density

$$E_{B,r} = \sum_e \int \frac{d^3k}{(2\pi)^3} \omega_k^e f_B(\omega_k^e) + \mu(n_0 + n_B). \quad (36)$$

At $T = 0$, we have $E_{B,r} = \mu n_0$, which is shown in the left panel of Fig. 3. We see that the bosonic energy density vanishes in the BCS regime because there is no Bose condensate in this case, $n_0 = 0$. In the far BEC regime, where $n_0 \neq 0$, the energy density vanishes too because the boson chemical potential, since coupled to the fermion chemical potential, vanishes. Only in the crossover region, where both the condensate and the chemical potential are nonzero, the energy density is nonvanishing.

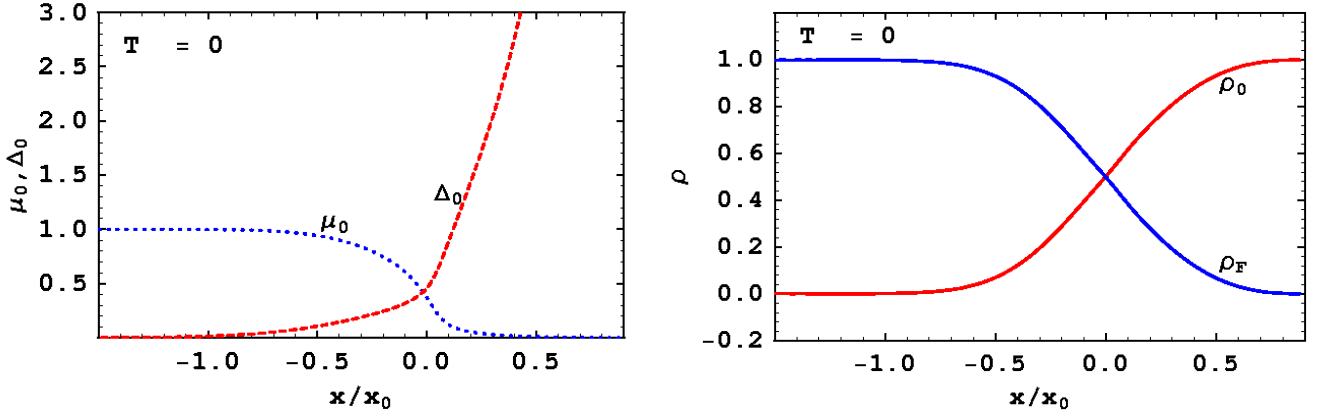


Figure 1: (Color online) Crossover at zero temperature from the BCS regime (small x) to the BEC regime (large x). Left panel: fermion chemical potential μ_0 (blue dotted) and gap Δ_0 (red dashed) in units of effective Fermi energy ϵ_F . Right panel: condensate fraction (red solid), fermion fraction (blue solid).

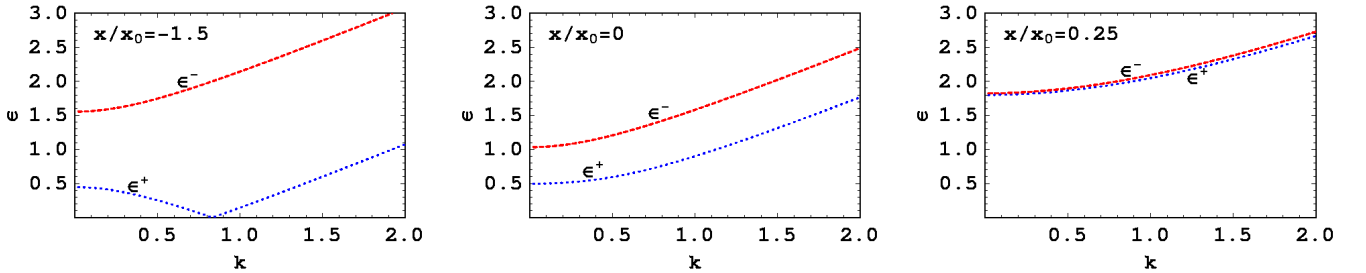


Figure 2: (Color online) Fermion and antifermion excitation energies ϵ_k^+ and ϵ_k^- as defined in Eq. (11) for three different values of the crossover parameter x/x_0 at $T = 0$ as a function of the momentum k (both ϵ_k^e and k are given in units of ϵ_F). In the BCS regime (left panel) the energy gap is small and the fermion excitations are well separated from antifermion excitations. Both excitations approach each other in the unitary regime (middle panel), and become indistinguishable in the far BEC regime (right panel). Note in particular that the minimum of the antiparticle excitation is not a monotonic function of x .

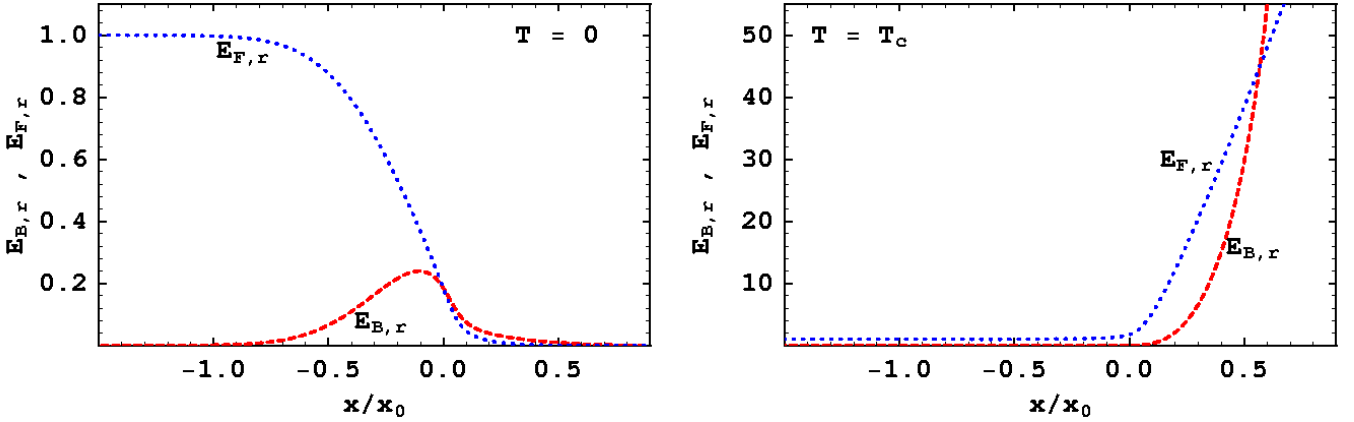


Figure 3: (Color online) Energy density of fermions and bosons in units of $\epsilon_F n$ at $T = 0$ (left panel) and at $T = T_c$ (right panel). In the BCS regime, $E_F = \epsilon_F n$ and $E_B = 0$ for all temperatures. The large fermionic and bosonic energy densities in the BEC regime at $T = T_c$ indicate the occupation of (quasi-)antiparticle modes.

B. Critical temperature

In this section, we calculate the critical temperature T_c and the corresponding particle densities as functions of x . Upon setting $\Delta = 0$ in the charge density equation (18) and the gap equation (28) one obtains

$$n = n_F + n_B, \quad (37a)$$

$$-x = \sum_{e=\pm} \int \frac{d^3 k}{(2\pi)^3} \left(\frac{1}{2\xi_k^e} \tanh \frac{\xi_k^e}{2T_c} - \frac{1}{2\epsilon_{k0}} \right), \quad (37b)$$

with the fermion density

$$n_F \equiv 2 \sum_{e=\pm} e \int \frac{d^3 k}{(2\pi)^3} f_F(\xi_k^e), \quad (38)$$

and the boson density given by Eq. (23). Strictly speaking, the original gap equation (28) is only valid for nonzero Δ (in its derivation, one has to divide by Δ). Therefore, Eq. (37b) has to be understood as a limit for approaching the critical temperature from below, $T \uparrow T_c$, i.e., for infinitesimally small Δ . Eqs. (37a) and (37b) can now be used to determine T_c and the corresponding chemical potential μ_c .

The results are shown in the left panel of Fig. 4. We see that the chemical potential behaves qualitatively as for zero temperature. The critical temperature, while exponentially small in the BCS regime, becomes of the order of and then larger than the chemical potential during the crossover. This is one of the characteristics of the strong coupling regime and one reason why this model (in its nonrelativistic version) is used to describe high-temperature superconductivity [20]. In Sec. III D we use the ratio T_c/Δ_0 to illustrate the high- T_c behavior.

The right panel of Fig. 4 shows the particle density fractions for fermions and bosons. A crossover similar to the zero-temperature case can be seen. The density fractions of fermions and bosons suggest that the crossover is shifted to a slightly larger value of x compared to the zero-temperature case. While at zero temperature $n_F = n_0$ occurs at $x/x_0 \simeq 0$, here we have $n_F = n_B$ at $x/x_0 \simeq 0.3$. It is clear that there is no Bose condensate at $T = T_c$; the bosonic population rather consists of thermal molecules. These are uncondensed, strongly-coupled Cooper pairs (see Ref. [26] for a recent discussion of this effect in the context of cold atoms). We see that uncondensed pairs do not exist in the BCS limit. In this case, the superfluid phase transition occurs “abruptly”, with pair formation and condensation at the same temperature.

In the right panel of Fig. 3 we show the fermion and boson energy densities. These curves are obtained by inserting the solutions for μ_c and T_c into Eq. (35) and (36) and making use of $\Delta = 0$. We see that, in contrast to the zero-temperature case, the fermionic energy density increases with x despite $n_F \rightarrow 0$. This is easy to understand from the corresponding quasi-fermion excitations. For all temperatures, the vanishing chemical potential renders quasi-particles and quasi-antiparticles degenerate. Whereas at $T = 0$ they are both gapped by Δ , at $T = T_c$ they are gapped only

by the fermion mass m . For large values of x we have $T_c \gg m$ and quasi-fermions as well as quasi-antifermions can be thermally excited. In this context, it would be interesting to consider the formation of chiral condensates which may be initiated by the degeneracy of quasi-fermions and quasi-antifermions. We leave this extension of the model for future studies.

The large increase of the bosonic energy density can be understood in the same way. Note, however, that, in contrast to the fermion mass, the boson mass decreases with increasing crossover parameter x . This difference, together with the different statistics of bosons and fermions gives rise to the qualitatively different behavior of $E_{B,r}$ compared to $E_{F,r}$. The strong increase of antiparticle densities has also been predicted in other models and has been termed “relativistic BEC (RBEC)” [15, 16].

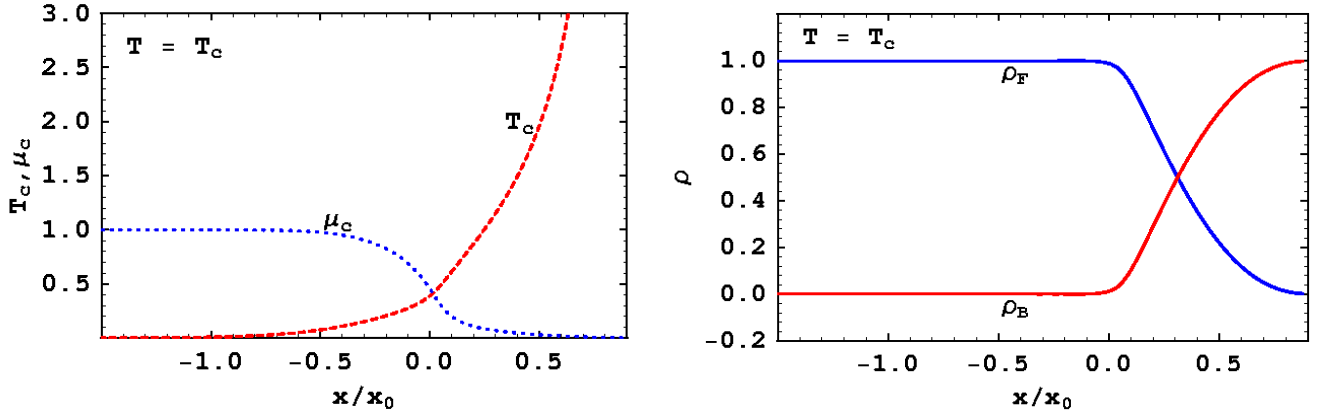


Figure 4: (Color online) Crossover at the critical temperature. Left panel: fermion chemical potential μ_c (blue dotted) and critical temperature T_c (red dashed) in units of the effective Fermi energy ϵ_F . Right panel: fermion fraction (blue solid), thermal boson fraction (red solid).

C. Fixed coupling

In the previous two subsections we have presented the solution of Eqs. (18) and (28) along two lines in the x - T plane: along the line $T = 0$ (Sec. III A) and along the (curved) line $T = T_c$ (Sec. III B). Now we explore a third path by fixing the crossover parameter and vary the temperature from zero to values beyond T_c . We shall use $x/x_0 = 0.2$ which is in the intermediate-coupling regime, where both fermionic and bosonic populations are present. For $T < T_c$, we use Eqs. (18) and (28) to determine μ and Δ . For $T > T_c$, the gap vanishes, $\Delta = 0$, i.e., we have the single equation (37a) to determine the chemical potential μ .

The condensate and the fermion and boson density fractions are shown in Fig. 5. At the left end, $T = 0$, one recovers the results shown in Fig. 1 at the particular value $x/x_0 = 0.2$, while the point $T/T_c = 1$ reproduces the respective result shown in Fig. 4. The second-order phase transition manifests itself in a kink in the density fractions and a vanishing condensate. Below T_c we observe coexistence of condensed bound states, condensed resonant states, and, for sufficiently large temperatures, uncondensed bound states. We obtain thermal bosons even above the phase transition. They can be interpreted as “preformed” pairs, just as the uncondensed pairs below T_c . This phenomenon is also called “pseudogap” in the literature [26, 27]. It suggests that there is a temperature $T^*(x)$ which marks the onset of pair formation. This temperature is not necessarily identical to T_c . In the BCS regime, $T^*(x) = T_c(x)$, while for $x \gtrsim 0$, $T^*(x) > T_c(x)$. Of course, our model does not predict any quantitative value for T^* because thermal bosons are present for all temperatures. Therefore, we expect the model to be valid only for a limited temperature range above T_c .

D. The ratios Δ_0/μ_0 and T_c/Δ_0

We finally present the results for the ratios Δ_0/μ_0 , and T_c/Δ_0 . They shall serve as a discussion of the dependence of our results on the boson-fermion coupling g and the fermion mass m . Both g and m were fixed throughout the

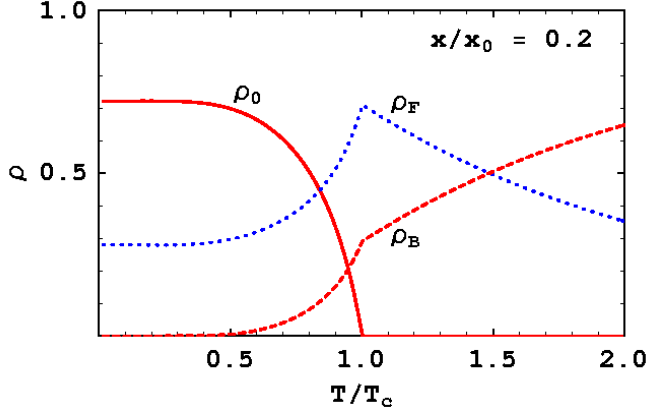


Figure 5: (Color online) Density fractions in the crossover regime at fixed $x/x_0 = 0.2$ as functions of temperature: condensed bosons (red solid), fermions and uncondensed bosons (blue dotted and red dashed, respectively).

previous sections. Moreover, we shall see that we reproduce values of these ratios obtained in different models in certain limit cases.

Fig. 6 shows the ratio Δ_0/μ_0 , using the results for Δ_0 and μ_0 from Sec. III A. From both panels one can read off the value of the ratio in the unitary limit, $x \rightarrow 0$. For the fermion mass that has been used in the previous subsections, $m/\Lambda = 0.2$, we find $1.2 \lesssim \Delta_0/\mu_0 \lesssim 1.4$. The exact value depends on the choice of g . This range is in agreement with nonrelativistic, purely fermionic models [22, 23, 24]. The right panel shows that the ratio in the unitary limit decreases with decreasing fermion mass. In particular, in the ultrarelativistic limit $m = 0$ we find $\Delta_0/\mu_0 \simeq 1.0$.

In Fig. 7 we show the ratio T_c/Δ_0 , using the result for T_c from Sec. III B. From BCS theory we know

$$\lim_{x \rightarrow -\infty} \frac{T_c}{\Delta_0} = \frac{e^\gamma}{\pi} \simeq 0.57, \quad (39)$$

where $\gamma \simeq 0.577$ is the Euler-Mascheroni constant. This value is reproduced in our results, independent of g and m . Upon increasing the crossover parameter x , the ratio deviates from its BCS value and increases substantially during the crossover where it strongly depends on the coupling g . Therefore we make no predictions for its value in the unitary regime. However, we see that in the BEC regime, the value again becomes independent of the parameters and assumes a value

$$\lim_{x \rightarrow x_0} \frac{T_c}{\Delta_0} \simeq 0.50. \quad (40)$$

IV. SUMMARY AND OUTLOOK

We have studied the relativistic BCS-BEC crossover for zero and nonzero temperatures within a boson-fermion model. Variations of this model have previously been used for nonrelativistic systems in order to study cold fermionic atoms and high-temperature superconductors. The bosons of the model are bound states of fermion pairs. Conversion of two fermions into a boson and vice versa is implemented by requiring chemical equilibrium with respect to this process. The crossover is realized by varying an effective coupling strength x , constructed from the difference between the renormalized boson mass $m_{b,r}$ and the boson chemical potential μ_b , and the boson-fermion coupling constant g , $x = -(m_{b,r}^2 - \mu_b^2)/(4g^2)$. In this form, $1/x$ plays the role of the scattering length, in particular $1/x = \pm\infty$ in the unitary limit. We have evaluated the model in its simplest form, employing a mean-field approximation and considering one single fermion species.

An important property of the model is the coexistence of weakly-coupled Cooper pairs with condensed and uncondensed bosonic bound states. In the crossover regime as well as in the BEC regime, strongly-bound molecular Cooper pairs exist below and above the critical temperature T_c . Above T_c , they are all uncondensed (“preformed” Cooper pairs) while below T_c a certain fraction of them forms a Bose-Einstein condensate. In contrast, in the BCS regime, pairing and condensation of fermionic degrees of freedom (in the absence of bosons) both set in at T_c .

Furthermore, we have characterized the onset of nonzero antifermion and antiboson populations during the crossover by computing the energy density. The reason for the appearance of antiparticles is the strong decrease of the fermion

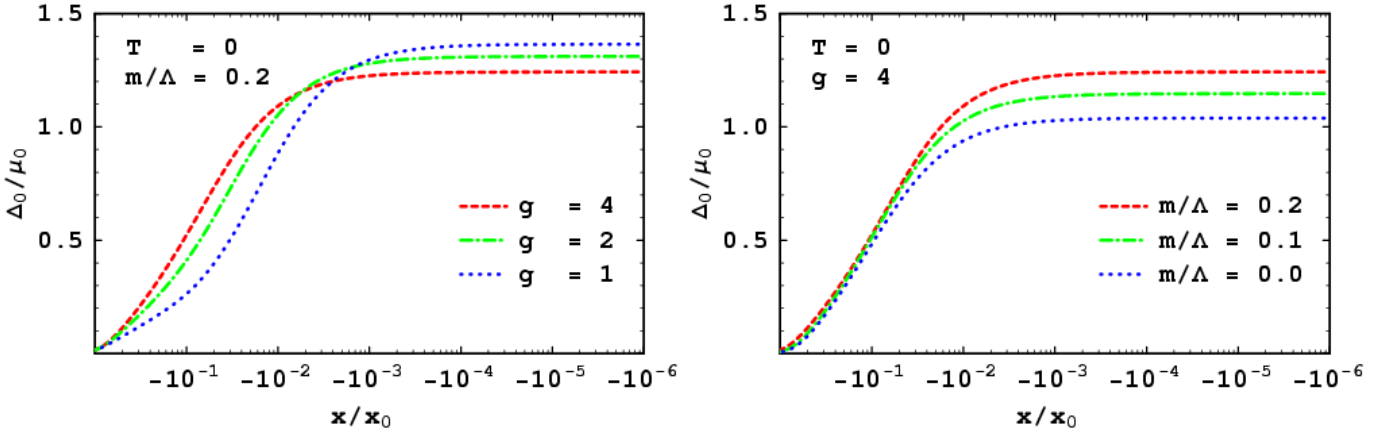


Figure 6: (Color online) Ratio of gap over chemical potential at zero temperature for crossover parameters $x/x_0 < 0$ on a logarithmic scale. The left end of the horizontal axis corresponds to the BCS regime, the right end, where $x \rightarrow 0$, corresponds to the unitary regime. Left panel: ratio for different values of the boson-fermion coupling g . Right panel: ratio for different values of the fermion mass.

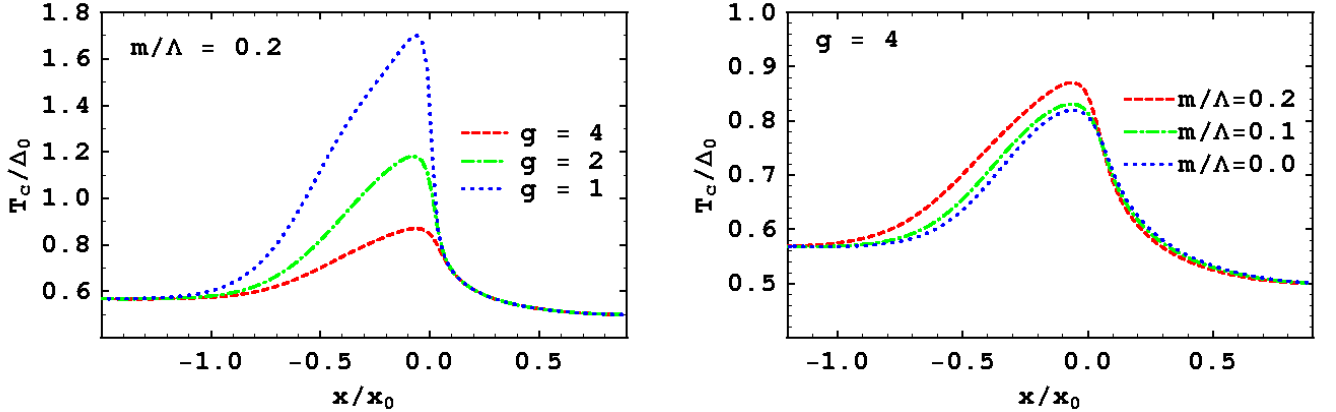


Figure 7: (Color online) Ratio of critical temperature over zero-temperature gap throughout the BCS-BEC crossover. Left panel: ratio for different values of the boson-fermion coupling g . Right panel: ratio for different values of the fermion mass.

chemical potential. While the fermion chemical potential is identical to the Fermi energy in the BCS regime, it reaches values well below the fermion mass in the BEC regime. As a consequence, particle and antiparticle excitation energies become almost identical and thus antiparticles are present for nonvanishing temperatures.

The model may be extended in several ways, in order to describe more realistic scenarios, for instance dense quark matter in the interior of a compact star. Besides going beyond the mean field approximation, one may straightforwardly introduce more than one fermion species. In particular, one may investigate the situation of pairing with mismatched number densities of two fermion species [28]. It would be interesting to study the influence of the uncondensed pairs on possible exotic superfluids in this situation. Moreover, chiral condensates can easily be integrated into the model.

Acknowledgments

A.S. acknowledges valuable discussions with M. Alford, S. Reddy, I. Shovkovy, and support by the U.S. Department of Energy under contracts DE-FG02-91ER50628 and DE-FG01-04ER0225 (OJI). Q.W. thanks P.-f. Zhuang for helpful discussions and is supported in part by the startup grant from University of Science and Technology of China (USTC) in association with 'Bai Ren' project of Chinese Academy of Sciences (CAS) and by National Natural Science Foundation

of China (NSFC) under the grant 10675109.

[1] J. Bardeen, L.N. Cooper, and J.R. Schrieffer, Phys. Rev. **108**, 1175 (1957).

[2] D. M. Eagles, Phys. Rev. **186**, 456 (1969); A. J. Leggett, in *Modern Trends in the Theory of Condensed Matter*, Springer-Verlag (1980); P. Nozieres and S. Schmitt-Rink, J. Low. Temp. Phys. **59**, 195 (1985).

[3] C.A. Regal, M. Greiner, and D.S. Jin, Phys. Rev. Lett. **92**, 040403 (2004) [arXiv:cond-mat/0401554]; M. Bartenstein *et. al.*, Phys. Rev. Lett. **92**, 120401 (2004) [arXiv:cond-mat/0401109]; M.W. Zwierlein *et. al.*, Phys. Rev. Lett. **92**, 120403 (2004) [arXiv:cond-mat/0403049]; J. Kinast *et. al.*, Phys. Rev. Lett. **92**, 150402 (2004) [arXiv:cond-mat/0403540]; T. Bourdel *et. al.*, Phys. Rev. Lett. **93**, 050401 (2004) [arXiv:cond-mat/0403091].

[4] M. W. Zwierlein, A. Schirotzek, C. H. Schunck and W. Ketterle, Science **311**, 492 (2006) [arXiv:cond-mat/0511197]; G. B. Partridge, W. Li, R. I. Kamar, Y. Liao and R. G. Hulet, Science **311**, 503 (2006) [arXiv:cond-mat/0511752].

[5] C.-H. Pao, S.-T. Wu, S.-K. Yip, Phys. Rev. B **73**, 132506 (2006) [arXiv:cond-mat/0506437]; D. T. Son and M. A. Stephanov, Phys. Rev. A **74**, 013614 (2006) [arXiv:cond-mat/0507586]; E. Gubankova, A. Schmitt and F. Wilczek, Phys. Rev. B **74**, 064505 (2006) [arXiv:cond-mat/0603603]; M. Mannarelli, G. Nardulli and M. Ruggieri, Phys. Rev. A **74**, 033606 (2006) [arXiv:cond-mat/0604579].

[6] D. T. Son and M. A. Stephanov, Phys. Rev. Lett. **86**, 592 (2001) [arXiv:hep-ph/0005225]; D. T. Son and M. A. Stephanov, Phys. Atom. Nucl. **64**, 834 (2001) [Yad. Fiz. **64**, 899 (2001)] [arXiv:hep-ph/0011365]; L. y. He, M. Jin and P. f. Zhuang, Phys. Rev. D **71**, 116001 (2005) [arXiv:hep-ph/0503272].

[7] J. C. Collins and M. J. Perry, Phys. Rev. Lett. **34**, 1353 (1975).

[8] B. C. Barrois, Nucl. Phys. B **129**, 390 (1977); D. Bailin and A. Love, Phys. Rept. **107**, 325 (1984).

[9] For reviews, see K. Rajagopal and F. Wilczek, arXiv:hep-ph/0011333; S. Reddy, Acta Phys. Polon. B **33**, 4101 (2002) [arXiv:nucl-th/0211045]; D. H. Rischke, Prog. Part. Nucl. Phys. **52**, 197 (2004) [arXiv:nucl-th/0305030]; M. Alford, Prog. Theor. Phys. Suppl. **153**, 1 (2004) [arXiv:nucl-th/0312007]; H. c. Ren, arXiv:hep-ph/0404074; M. Huang, Int. J. Mod. Phys. E **14**, 675 (2005) [arXiv:hep-ph/0409167]; I. A. Shovkovy, Found. Phys. **35**, 1309 (2005) [arXiv:nucl-th/0410091]; T. Schäfer, arXiv:hep-ph/0509068.

[10] D. T. Son, Phys. Rev. D **59**, 094019 (1999) [arXiv:hep-ph/9812287]; D. K. Hong, V. A. Miransky, I. A. Shovkovy and L. C. R. Wijewardhana, Phys. Rev. D **61**, 056001 (2000) [Erratum-ibid. D **62**, 059903 (2000)] [arXiv:hep-ph/9906478]; W. E. Brown, J. T. Liu and H. c. Ren, Phys. Rev. D **61**, 114012 (2000) [arXiv:hep-ph/9908248]; R. D. Pisarski and D. H. Rischke, Phys. Rev. D **61**, 074017 (2000) [arXiv:nucl-th/9910056].

[11] For recent developments in color superconductivity using perturbative QCD, see Q. Wang and D. H. Rischke, Phys. Rev. D **65**, 054005 (2002) [arXiv:nucl-th/0110016]; A. Schmitt, Q. Wang and D. H. Rischke, Phys. Rev. D **66**, 114010 (2002) [arXiv:nucl-th/0209050]; A. Ipp, A. Gerhold and A. Rebhan, Phys. Rev. D **69**, 011901 (2004) [arXiv:hep-ph/0309019]; Q. Wang, J. Phys. G **30**, S1251 (2004) [arXiv:nucl-th/0404017]; P. T. Reuter, Q. Wang and D. H. Rischke, Phys. Rev. D **70**, 114029 (2004) [Erratum-ibid. D **71**, 099901 (2005)] [arXiv:nucl-th/0405079]; A. Gerhold and A. Rebhan, Phys. Rev. D **71**, 085010 (2005) [arXiv:hep-ph/0501089]; P. T. Reuter, arXiv:nucl-th/0602043; J. L. Noronha, H. c. Ren, I. Giannakis, D. Hou and D. H. Rischke, Phys. Rev. D **73**, 094009 (2006) [arXiv:hep-ph/0602218]; D. Nickel, J. Wambach and R. Alkofer, Phys. Rev. D **73**, 114028 (2006) [arXiv:hep-ph/0603163]; B. Feng, D. f. Hou, J. r. Li and H. c. Ren, Nucl. Phys. B **754**, 351 (2006) [arXiv:nucl-th/0606015]; P. T. Reuter, Phys. Rev. D **74**, 105008 (2006) [arXiv:nucl-th/0608020].

[12] M. Buballa, Phys. Rept. **407**, 205 (2005) [arXiv:hep-ph/0402234]; S. B. Rüster, V. Werth, M. Buballa, I. A. Shovkovy and D. H. Rischke, Phys. Rev. D **72**, 034004 (2005) [arXiv:hep-ph/0503184].

[13] K. Nawa, E. Nakano and H. Yabu, Phys. Rev. D **74**, 034017 (2006) [arXiv:hep-ph/0509029]; A. H. Rezaeian and H. J. Pirner, Nucl. Phys. A **779**, 197 (2006) [arXiv:nucl-th/0606043].

[14] M. Kitazawa, D. H. Rischke and I. A. Shovkovy, Phys. Lett. B **637**, 367 (2006) [arXiv:hep-ph/0602065].

[15] Y. Nishida and H. Abuki, Phys. Rev. D **72**, 096004 (2005) [arXiv:hep-ph/0504083].

[16] H. Abuki, arXiv:hep-ph/0605081.

[17] K. Rajagopal and A. Schmitt, Phys. Rev. D **73**, 045003 (2006) [arXiv:hep-ph/0512043].

[18] R. Friedberg and T. D. Lee, Phys. Rev. B **40**, 6745 (1989); R. Friedberg, T. D. Lee and H. C. Ren, Phys. Rev. B **42**, 4122 (1990).

[19] M. Holland, S.J.J.M.F. Kokkelmans, M.L. Chiofalo, R. Walser, Phys. Rev. Lett. **87**, 120406 (2001) [arXiv:cond-mat/0103479]; M.L. Chiofalo, S.J.J.M.F. Kokkelmans, J.N. Milstein, M.J. Holland, Phys. Rev. Lett. **88**, 090402 (2001) [arXiv:cond-mat/0110119]; E. Timmermans, K. Furuya, P.W. Milonni, A.K. Kerman, Phys. Lett. A **285**, 228 (2001) [arXiv:cond-mat/0103327]; Y. Ohashi and A. Griffin, Phys. Rev. Lett. **89**, 130402 (2002).

[20] J. Ranninger in *Bose-Einstein condensation*, edited by A. Griffin, D.W. Snoke, and S. Stringari (Cambridge University Press, Cambridge, 1995); T. Domanski, J. Ranninger, Physica C **387**, 77 (2003) [arXiv:cond-mat/0208255].

[21] J.I. Kapusta, *Finite-temperature field theory* (Cambridge University Press, Cambridge, 1989).

[22] S.Y. Chang, J. Carlson, V.R. Pandharipande, K.E. Schmidt, Phys. Rev. A. **70**, 043602 (2004) [arXiv:physics/0404115].

[23] J. Carlson and S. Reddy, Phys. Rev. Lett. **95**, 060401 (2005) [arXiv:cond-mat/0503256].

[24] Y. Nishida and D. T. Son, Phys. Rev. Lett. **97**, 050403 (2006) [arXiv:cond-mat/0604500]; A. Bulgac and M. M. Forbes, arXiv:cond-mat/0606043; G. Rupak, T. Schäfer and A. Kryjevski, arXiv:cond-mat/0607834; Y. Nishida and D. T. Son, arXiv:cond-mat/0607835.

- [25] M. Alford and Q. h. Wang, J. Phys. G **31**, 719 (2005) [arXiv:hep-ph/0501078].
- [26] Q. Chen, J. Stajic, S. Tan, K. Levin, Phys. Rep. **412**, 1 (2005); K. Levin, Q. Chen, arXiv:cond-mat/0610006.
- [27] M. Kitazawa, T. Koide, T. Kunihiro and Y. Nemoto, Prog. Theor. Phys. **114**, 117 (2005) [arXiv:hep-ph/0502035]; M. Kitazawa, T. Kunihiro and Y. Nemoto, Phys. Lett. B **631**, 157 (2005) [arXiv:hep-ph/0505070].
- [28] J. Deng, A. Schmitt and Q. Wang, in preparation.